Progress In Electromagnetics Research M, Vol. 38, 15–24, 2014

Orbital Angular Momentum Density of a Hollow Vortex Gaussian Beam

Yimin Zhou and Guoquan Zhou*

Abstract—Here the hollow vortex Gaussian beam is described by the exact solution of the Maxwell equations. By means of the method of the vectorial angular spectrum, analytical expressions of the electromagnetic fields of a hollow vortex Gaussian beam propagating in free space are derived. By using the electromagnetic fields of a hollow vortex Gaussian beam beyond the paraxial approximation, one can calculate the orbital angular momentum density distribution of a hollow vortex Gaussian beam in free space. The overall transverse components of the orbital angular momentum of a hollow vortex Gaussian beam are equal to zero. Therefore, the influences of the topological charge, beam order, Gaussian waist size, and linearly polarized angle on the distribution of longitudinal component of the orbital angular momentum density of a hollow vortex Gaussian beam are numerically demonstrated in the reference plane. The outcome is useful to optical trapping, optical guiding, and optical manipulation using the hollow vortex Gaussian beams.

1. INTRODUCTION

Dark hollow beams have important application prospect in atom optics for their specific performance. Therefore, dark hollow beams become one of the most interesting topics in optics and lasers [1–3]. Many beam models have been constructed to mathematically describe dark hollow laser beams [4–7]. Also, dark hollow beams can be experimentally realized by means of differently ingenious methods [8–11]. The properties of dark hollow beams have been extensively investigated [12–16]. Focusing of dark hollow Gaussian electromagnetic beams has been studied in a plasma with relativistic–ponderomotive regime [17]. Upon propagation, the previous beam models are unstable. In other words, the dark region in the previous beam models will disappear upon propagation. This phenomenon can be interpreted as follows. These beam models are described by the superposition of different laser modes. Upon propagation, the dark region will turn into the bright region, which is caused by the interference of these differently propagating laser modes. To overcome this defect, a kind of hollow vortex Gaussian beams has been recently introduced [18], and the dark region in the hollow vortex Gaussian beam still exists during propagation.

Carrying the orbital angular momentum, the hollow vortex Gaussian beam has many potential applications in optical trapping, optical micro-manipulation, nonlinear optics, and quantum information processing [19–22]. When the hollow vortex Gaussian beam interacts with microscopic particles, the orbital angular momentum in the hollow vortex Gaussian beam can be exchanged to microscopic particles. Therefore, here we investigate the distribution of the orbital angular momentum density of a hollow vortex Gaussian beam. Moreover, the starting point to describe a hollow vortex Gaussian beam is the Maxwell equations in free space. To obtain the exact solution of the Maxwell equations, we use the method of vectorial angular spectrum. By using the electromagnetic field of a hollow vortex Gaussian beam beyond the paraxial approximation, the expression of the orbital angular momentum density of a hollow vortex Gaussian beam propagating in free space is derived. The effects of the beam

Received 6 June 2014, Accepted 4 August 2014, Scheduled 10 August 2014
* Corresponding author: Guoquan Zhou (zhouguoquan178@sohu.com).
The authors are with the School of Sciences, Zhejiang A & F University, Lin'an 311300, China.

parameters on the distribution of the orbital angular momentum density of a hollow vortex Gaussian beam are discussed by numerical simulations.

2. ORBITAL ANGULAR MOMENTUM DENSITY OF A HOLLOW VORTEX GAUSSIAN BEAM

In the cylindrical coordinate system, z-axis is the propagation axis, and plane $z = 0$ is the source plane. The hollow vortex Gaussian beam in the source plane is described by [17]

$$\begin{bmatrix} E_x(\rho_0, 0) \\ E_y(\rho_0, 0) \end{bmatrix} = \begin{pmatrix} \cos\alpha \\ \sin\alpha \end{pmatrix} \frac{\rho_0^{2n}}{w_0^{2n}} \exp\left(-\frac{\rho_0^2}{w_0^2}\right) \exp(im\theta_0), \tag{1}$$

where $\rho_0 = (x_0^2 + y_0^2)^{1/2}$ and $\theta_0 = \arctan(y_0/x_0)$. w_0 is the Gaussian waist size, n the beam order, and m the topological charge. For simplicity, here m is assumed to be positive. $\begin{pmatrix} \cos\alpha \\ \sin\alpha \end{pmatrix}$ describes the linearly polarized state, and α is the linearly polarized angle. Here the description of a hollow vortex Gaussian beam is started from the Maxwell equations [23, 24]:

$$\nabla \times \mathbf{E}(\rho, z) - \mathbf{i}k\mathbf{H}(\rho, z) = 0, \tag{2}$$

$$\nabla \times \mathbf{H}(\rho, z) + \mathbf{i}k\mathbf{E}(\rho, z) = 0, \tag{3}$$

$$\nabla \cdot \mathbf{E}(\rho, z) = \nabla \cdot \mathbf{H}(\rho, z) = 0, \tag{4}$$

where $\rho = (x^2 + y^2)^{1/2}$ and $k = 2\pi/\lambda$ is the wave number with λ being the optical wavelength. $\mathbf{E}(\rho, z)$ and $\mathbf{H}(\rho, z)$ are electric and magnetic fields, respectively. In frequency domain, the Maxwell equations can be rewritten as

$$\mathbf{L} \times \tilde{\mathbf{E}}(b, z) - \mathbf{i}k\tilde{\mathbf{H}}(b, z) = 0 \tag{5}$$

$$\mathbf{L} \times \tilde{\mathbf{H}}(b, z) + \mathbf{i}k\tilde{\mathbf{E}}(b, z) = 0, \tag{6}$$

$$\mathbf{L} \cdot \bar{\mathbf{E}}(b, z) = L \cdot \tilde{\mathbf{H}}(b, z) = 0 \tag{7}$$

where $\mathbf{L} = \mathbf{i}kp\mathbf{e}_x + ikq\mathbf{e}_y + \frac{\partial}{\partial z}\mathbf{e}_z$ and $b = (p^2 + q^2)^{1/2}$. $\mathbf{e}_x$, $\mathbf{e}_y$, and $\mathbf{e}_z$ are three unit vectors of the rectangular coordinate system. p/λ and q/λ are the transverse frequencies. $\mathbf{E}(\rho, z)$ and $\mathbf{H}(\rho, z)$ can be obtained by the Fourier transform of $\tilde{\mathbf{E}}(b, z)$ and $\tilde{\mathbf{H}}(b, z)$:

$$\mathbf{E}(\rho, z) = \int_{-\infty}^{\infty}\int_{-\infty}^{\infty} \tilde{\mathbf{E}}(b, z) \exp[\mathbf{i}k(px + qy)]dpdq, \tag{8}$$

$$\mathbf{H}(\rho, z) = \int_{-\infty}^{\infty}\int_{-\infty}^{\infty} \tilde{\mathbf{H}}(b, z) \exp[\mathbf{i}k(px + qy)]dpdq, \tag{9}$$

Eqs. (5)–(7) have the following solutions:

$$\tilde{\mathbf{E}}(b, z) = \mathbf{A}(p, q) \exp(\mathbf{i}k\gamma z), \tag{10}$$

$$\tilde{\mathbf{H}}(b, z) = [\mathbf{s} \times \mathbf{A}(p, q)] \exp(\mathbf{i}k\gamma z), \tag{11}$$

where $\mathbf{s} = p\mathbf{e}_x + q\mathbf{e}_y + \gamma\mathbf{e}_z$ and $\gamma = (1 - b^2)^{1/2}$. $\mathbf{A}(p, q) = A_x(p, q)\mathbf{e}_x + A_y(p, q)\mathbf{e}_y + A_z(p, q)\mathbf{e}_z$ is the vectorial angular spectrum. $A_x(p, q)$ and $A_y(p, q)$ are given by

$$\begin{aligned} \begin{bmatrix} A_x(p, q) \\ A_y(p, q) \end{bmatrix} &= \frac{1}{\lambda^2}\int_{-\infty}^{\infty}\int_{-\infty}^{\infty} \begin{bmatrix} E_x(\rho_0, z) \\ E_y(\rho_0, z) \end{bmatrix} \exp[-ik(px_0 + qy_0)]dx_0dy_0 \\ &= \begin{pmatrix} \cos\alpha \\ \sin\alpha \end{pmatrix} \frac{1}{\lambda^2}\int_0^{\infty}\int_0^{2\pi} \frac{\rho_0^{2n}}{w_0^{2n}} \exp\left(-\frac{\rho_0^2}{w_0^2}\right) \exp[im\theta_0 - ikb\rho_0\cos(\theta_0 - \varphi)]\rho_0 d\rho_0 d\theta_0, \end{aligned} \tag{12}$$

where $\varphi = \arctan(q/p)$. We recall the following mathematical formulae [25]:

$$J_m(x) = \frac{(-i)^m}{2\pi}\int_0^{2\pi} \exp(ix\cos\theta_0 + im\theta_0)d\theta_0, \tag{13}$$

$$\int_0^{\infty} x^{n-1}\exp\left(-x^2\right) J_m(\alpha x)dx = \frac{\alpha^m}{2^{m+1}m!}\Gamma\left(\frac{n+m}{2}\right)\exp\left(-\frac{\alpha^2}{4}\right){}_1F_1\left(\frac{m-n}{2}+1; m+1; \frac{\alpha^2}{4}\right), \tag{14}$$

where J_m is the m-th order Bessel function of the first kind, $\Gamma(\cdot)$ a Gamma function, and ${}_1F_1(\cdot;\cdot;\cdot)$ a Kummer function and defined by [25]

$$ {}_1F_1(u;v;x) = \frac{\Gamma(v)}{\Gamma(u)} \sum_{l=0}^{\infty} \frac{\Gamma(l+u)}{\Gamma(l+v)} \frac{x^l}{l!}. \tag{15} $$

The transversal components of the vectorial angular spectrum are found to be

$$ \begin{aligned} \begin{bmatrix} A_x(p,q) \\ A_y(p,q) \end{bmatrix} &= \begin{pmatrix} \cos\alpha \\ \sin\alpha \end{pmatrix} \frac{(-i)^m}{\pi m! 2^{m+2} f^{m+2}} \Gamma\left(n+1+\frac{m}{2}\right) b^m \\ &\quad \exp\left(-\frac{b^2}{4f^2}\right) {}_1F_1\left(\frac{m}{2}-n; m+1; \frac{b^2}{4f^2}\right) \exp(im\varphi), \end{aligned} \tag{16} $$

where $f = 1/(kw_0)$. The longitudinal component $A_z(p,\ q)$ is given by the orthogonal relation $s \cdot A(p,q) = 0$ and turns out to be

$$ A_z(p,q) = -b[A_x(p,q)\cos\varphi + A_y(p,q)\sin\varphi]/\gamma. \tag{17} $$

The propagating optical field of a hollow vortex Gaussian beam in the z-plane can be expressed in the form of the vectorial angular spectrum:

$$ \begin{aligned} \mathbf{E}(\rho,z) &= \int_0^{\infty}\int_0^{2\pi} \left[A_x(p,q)\left(\mathbf{e}_x - \frac{b\cos\varphi}{\gamma}\mathbf{e}_z\right) + A_y(p,q)\left(\mathbf{e}_y - \frac{b\sin\varphi}{\gamma}\mathbf{e}_z\right)\right] \\ &\quad \exp\{ik[b\rho\cos(\varphi-\theta)+\gamma z]\}\, bdbd\varphi, \end{aligned} \tag{18} $$

where $\theta = \arctan(y/x)$. Also, the propagating optical field of a hollow vortex Gaussian beam can be expressed as

$$ \mathbf{E}(\rho,z) = E_x(\rho,z)\mathbf{e}_x + E_y(\rho,z)\mathbf{e}_y + E_z(\rho,z)\mathbf{e}_z. \tag{19} $$

The x-component of the optical field of a hollow vortex Gaussian beam reads as

$$ \begin{aligned} E_x(\rho,z) &= \frac{\cos\alpha}{2f^2}\exp(im\theta)\frac{\Gamma(n+1+0.5m)}{\Gamma(0.5m-n)} \sum_{l=0}^{\infty} \frac{\Gamma(l+0.5m-n)}{l!(l+m)!} \int_0^{\infty} \left(\frac{b}{2f}\right)^{m+2l} \exp\left(-\frac{b^2}{4f^2}\right) \\ &\quad \times J_m(kb\rho)\exp(ik\gamma z) bdb. \end{aligned} \tag{20} $$

Normally, the reference plane where the hollow vortex Gaussian beam is practically used is $z > \lambda$. In the case of $z > \lambda$, the effect of the evanescent waves can be ignored. When $z > \lambda$, therefore, the upper integral limit in Eq. (20) can be replaced by 1. In this case, $\exp(ik\gamma z)$ can be expanded as [25]

$$ \exp(ik\gamma z) = \sum_{s=0}^{\infty} \frac{1}{2^s s!} (kz)^{s+1} H_{s-1}^1(kz) b^{2s}, \tag{21} $$

where H_{s-1}^1 is the $(s-1)$th–order spherical Bessel function of the third kind. The x-component of the optical field of a hollow vortex Gaussian beam is found to be

$$ \begin{aligned} E_x(\rho,z) &= \frac{\cos\alpha}{2f^2}\exp(im\theta)\frac{\Gamma(n+1+0.5m)}{\Gamma(0.5m-n)} \sum_{l=0}^{\infty}\sum_{s=0}^{\infty} \frac{\Gamma(l+0.5m-n)}{s!l!(l+m)!} 2^s f^{2s} (kz)^{s+1} H_{s-1}^1(kz) \\ &\quad \times \left(\int_0^{\infty} - \int_1^{\infty}\right) \left(\frac{b}{2f}\right)^{m+2l+2s} \exp\left(-\frac{b^2}{4f^2}\right) J_m(kb\rho) bdb. \end{aligned} \tag{22} $$

When $b > 1$, the integrands decay exponentially. Therefore, the second integral can be negligible. The x-component of the optical field of a hollow vortex Gaussian beam analytically yields

$$ \begin{aligned} E_x(\rho,z) &= \cos\alpha \frac{\Gamma(n+1+0.5m)}{\Gamma(0.5m-n)} \left(\frac{\rho}{w_0}\right)^m \exp\left(-\frac{\rho^2}{w_0^2}\right)\exp(im\theta) \\ &\quad \times \sum_{l=0}^{\infty}\sum_{s=0}^{\infty} \frac{\Gamma(l+0.5m-n)(l+s)!}{s!l!(l+m)!} 2^s f^{2s} (kz)^{s+1} H_{s-1}^1(kz) L_{l+s}^m\left(\frac{\rho^2}{w_0^2}\right), \end{aligned} \tag{23} $$

where $L_{l+s}^{m}(\cdot)$ is the associated Laguerre polynomial. Similarly, the y-component of the optical field of a hollow vortex Gaussian beam is given by

$$\begin{aligned} E_y(\rho,z) &= \sin\alpha\frac{\Gamma(n+1+0.5m)}{\Gamma(0.5m-n)}\left(\frac{\rho}{w_0}\right)^m\exp\left(-\frac{\rho^2}{w_0^2}\right)\exp(im\theta) \\ &\times\sum_{l=0}^{\infty}\sum_{s=0}^{\infty}\frac{\Gamma(l+0.5m-n)(l+s)!}{s!l!(l+m)!}2^s f^{2s}(kz)^{s+1}H_{s-1}^{1}(kz)L_{l+s}^{m}\left(\frac{\rho^2}{w_0^2}\right). \end{aligned} \tag{24}$$

The longitudinal component of the optical field of a hollow vortex Gaussian beam turns out to be

$$\begin{aligned} E_z(\rho,z) &= -\frac{i\Gamma(n+1+0.5m)}{2f^2\Gamma(0.5m-n)}\exp(im\theta)(\cos\alpha\cos\theta+\sin\alpha\sin\theta)\sum_{l=0}^{\infty}\frac{\Gamma(l+0.5m-n)}{l!(l+m)!} \\ &\times\int_0^{\infty}\left(\frac{b}{2f}\right)^{m+2l}\exp\left(-\frac{b^2}{4f^2}\right)J_{m+1}(k\rho b)\frac{b}{\gamma}\exp(ik\gamma z)bdb. \end{aligned} \tag{25}$$

When $b<1$, the following expansion is valid [25]

$$\frac{\exp(ik\gamma z)}{\gamma}=\sum_{s=0}^{\infty}\frac{i}{2^s s!}(kz)^{s+1}H_s^1(kz)b^{2s}. \tag{26}$$

The longitudinal component of the optical field of a hollow vortex Gaussian beam can be analytically expressed as

$$\begin{aligned} E_z(\rho,z) &= \frac{\Gamma(n+1+0.5m)}{2\Gamma(0.5m-n)}\left(\frac{\rho}{w_0}\right)^{m+1}\exp\left(-\frac{\rho^2}{w_0^2}\right)\{(\cos\alpha-i\sin\alpha)\exp[i(m+1)\theta]+(\cos\alpha+i\sin\alpha) \\ &\times\exp[i(m-1)\theta]\}\sum_{l=0}^{\infty}\sum_{s=0}^{\infty}\frac{\Gamma(l+0.5m-n)(l+s)!}{s!l!(l+m)!}2^{s+1}f^{2s+1}(kz)^{s+1}H_s^1(kz)L_{l+s}^{m+1}\left(\frac{\rho^2}{w_0^2}\right) \end{aligned} \tag{27}$$

Upon propagation, the longitudinal component of the optical field of the hollow vortex Gaussian beam is a mixed mode of the $(m+1)$-order topological charge and the $(m-1)$-order topological charge.

One can obtain the magnetic field of a hollow vortex Gaussian beam by

$$\mathbf{H}(\rho,z)=\frac{1}{i\omega\mu_0}\nabla\times\mathbf{E}(\rho,z), \tag{28}$$

where μ_0 is the magnetic permeability of vacuum. The Poyting vector of a hollow vortex Gaussian beam reads as

$$\mathbf{S}(\rho,z)=\frac{1}{4}<\mathbf{E}(\rho,z)\times\mathbf{H}^*(\rho,z)+\mathbf{E}^*(\rho,z)\times\mathbf{H}(\rho,z)>=S_x(\rho,z)\mathbf{e}_x+S_y(\rho,z)\mathbf{e}_y+S_z(\rho,z)\mathbf{e}_z, \tag{29}$$

with $S_x(\rho,z)$, $S_y(\rho,z)$, and $S_z(\rho,z)$ being given by

$$\begin{aligned} S_x(\rho,z) &= \frac{1}{4i\omega\mu_0}\left\{E_y^*(\rho,z)\left[\frac{\partial E_y(\rho,z)}{\partial x}-\frac{\partial E_x(\rho,z)}{\partial y}\right]+E_z(\rho,z)\left[\frac{\partial E_x^*(\rho,z)}{\partial z}-\frac{\partial E_z^*(\rho,z)}{\partial x}\right]\right. \\ &\left.-E_y(\rho,z)\left[\frac{\partial E_y^*(\rho,z)}{\partial x}-\frac{\partial E_x^*(\rho,z)}{\partial y}\right]-E_z^*(\rho,z)\left[\frac{\partial E_x(\rho,z)}{\partial z}-\frac{\partial E_z(\rho,z)}{\partial x}\right]\right\}, \end{aligned} \tag{30}$$

$$\begin{aligned} S_y(\rho,z) &= \frac{1}{4i\omega\mu_0}\left\{E_x(\rho,z)\left[\frac{\partial E_y^*(\rho,z)}{\partial x}-\frac{\partial E_x^*(\rho,z)}{\partial y}\right]+E_z^*(\rho,z)\left[\frac{\partial E_z(\rho,z)}{\partial y}-\frac{\partial E_y(\rho,z)}{\partial z}\right]\right. \\ &\left.-E_z(\rho,z)\left[\frac{\partial E_z^*(\rho,z)}{\partial y}-\frac{\partial E_y^*(\rho,z)}{\partial z}\right]-E_x^*(\rho,z)\left[\frac{\partial E_y(\rho,z)}{\partial x}-\frac{\partial E_x(\rho,z)}{\partial y}\right]\right\}, \end{aligned} \tag{31}$$

$$\begin{aligned} S_z(\rho,z) &= \frac{1}{4i\omega\mu_0}\left\{E_x^*(\rho,z)\left[\frac{\partial E_x(\rho,z)}{\partial z}-\frac{\partial E_z(\rho,z)}{\partial x}\right]+E_y(\rho,z)\left[\frac{\partial E_z^*(\rho,z)}{\partial y}-\frac{\partial E_y^*(\rho,z)}{\partial z}\right]\right. \\ &\left.-E_x(\rho,z)\left[\frac{\partial E_x^*(\rho,z)}{\partial z}-\frac{\partial E_z^*(\rho,z)}{\partial x}\right]-E_y^*(\rho,z)\left[\frac{\partial E_z(\rho,z)}{\partial y}-\frac{\partial E_y(\rho,z)}{\partial z}\right]\right\}, \end{aligned} \tag{32}$$

where the angle brackets denote an average to the time, and the asterisk indicates the complex conjugation. Therefore, the orbital angular momentum density of a hollow vortex Gaussian beam turns out to be [26, 27]

$$\mathbf{J}(\rho,z)=\varepsilon_0\mu_0[\mathbf{r}\times\mathbf{S}(\rho,z)]=J_x(\rho,z)\mathbf{e}_x+J_y(\rho,z)\mathbf{e}_y+J_z(\rho,z)\mathbf{e}_z, \tag{33}$$

with $J_x(\rho,\, z)$, $J_y(\rho,\, z)$, and $J_z(\rho,\, z)$ being given by

$$J_x(\rho,z) = \varepsilon_0\mu_0[yS_z(\rho,z)-zS_y(\rho,z)], \tag{34}$$
$$J_y(\rho,z) = \varepsilon_0\mu_0[zS_x(\rho,z)-xS_z(\rho,z)], \tag{35}$$
$$J_z(\rho,z) = \varepsilon_0\mu_0[xS_y(\rho,z)-yS_x(\rho,z)], \tag{36}$$

where $\mathbf{r}=x\mathbf{e}_x+y\mathbf{e}_y+z\mathbf{e}_z$ and ε_0 is the electric permittivity of vacuum. Inserting Eqs. (23), (24), and (27) into Eqs. (34)–(36), one can calculate the orbital angular momentum density of a hollow vortex Gaussian beam.

3. NUMERICAL CALCULATIONS AND ANALYSES

The x- and the y-components of the orbital angular momentum density of a hollow vortex Gaussian beam in the reference plan $z=25\lambda$ are shown in Figs. 1 and 2 where $w_0=5\lambda$, $n=2$, and $m=1$. In subfigures (a)–(d), $\alpha=0$, $\pi/4, \pi/3$, and $\pi/2$, respectively. The x-component of the angular momentum density is composed of two lobes, which is closely located in the vertical direction. The areas of the two lobes are equivalent. However, the signs of the angular momentum density in the two lobes are opposite. Accordingly, the overall x-component of the angular momentum in the reference plane is zero. The y-component of the angular momentum density is composed of two lobes too, which are closely located in the horizontal direction. Also, the overall y-component of the angular momentum in the reference plane is zero. The overall traversal components of the orbital angular momentum are confirmed to be zero. Therefore, hereafter we only consider the longitudinal component of the orbital angular momentum density.

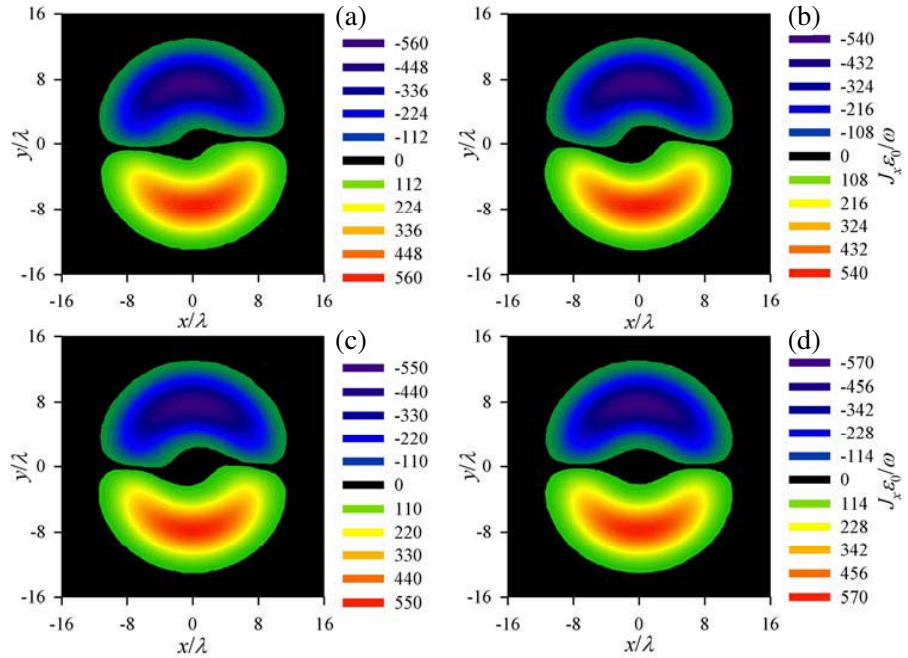

Figure 1. The x-component of the orbital angular momentum density of a hollow vortex Gaussian beam in the reference plan $z=25\lambda$. $w_0=5\lambda$, $n=2$, and $m=1$. (a) $\alpha=0$. (b) $\alpha=\pi/4$. (c) $\alpha=\pi/3$. (d) $\alpha=\pi/2$.

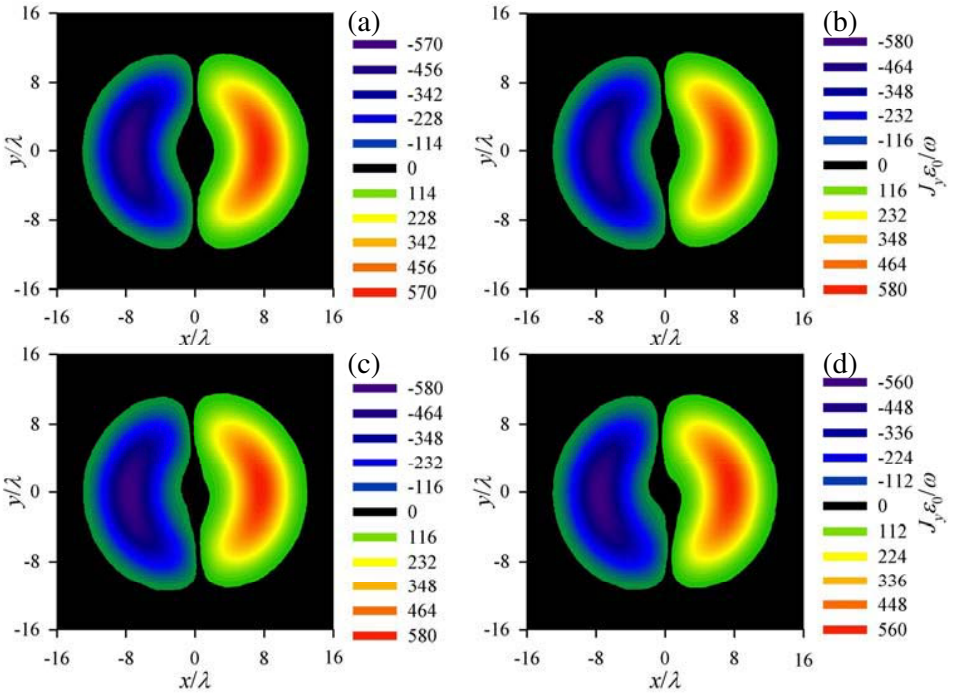

Figure 2. The y-component of the orbital angular momentum density of a hollow vortex Gaussian beam in the reference plan $z = 25\lambda$. $w_0 = 5\lambda$, $n = 2$, and $m = 1$. (a) $\alpha = 0$. (b) $\alpha = \pi/4$. (c) $\alpha = \pi/3$. (d) $\alpha = \pi/2$.

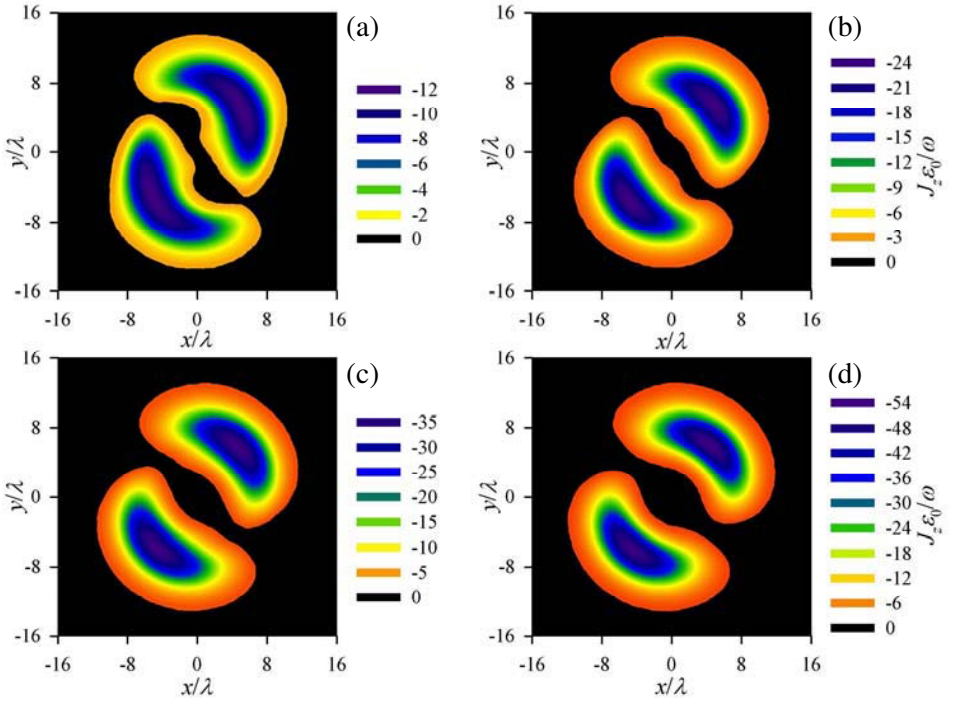

Figure 3. The longitudinal component of the orbital angular momentum density of a hollow vortex Gaussian beam in the reference plan $z = 25\lambda$. $w_0 = 5\lambda$, $n = 2$, and $\alpha = \pi/4$. (a) $m = 1$. (b) $m = 2$. (c) $m = 3$. (d) $m = 4$.

The orbital angular momentum density of a hollow vortex Gaussian beam in a reference plane depends on the topological charge, beam order, Gaussian waist size, and linearly polarized angle. Now, we examine the effects of these four parameters on the distribution of the orbital angular momentum density. The reference plane is fixed to be $z = 25\lambda$. First, the influence of the topological charge on the distribution of the orbital angular momentum density is considered, which is shown in Fig. 3 where $w_0 = 5\lambda$, $n = 2$, and $\alpha = \pi/4$. The longitudinal component of the angular momentum density is always negative. The negative angular momentum density indicates that the corresponding spiral direction is opposite to that of the positive angular momentum density. With increasing the topological charge, the magnitude of the longitudinal component of the angular momentum density augments, which results in the overall orbital angular momentum also augmenting. With altering the topological charge, the profile of the longitudinal component of the angular momentum density also changes slightly. Fig. 4 shows the effect of the beam order on the distribution of the orbital angular momentum density with $w_0 = 5\lambda$, $m = 3$, and $\alpha = \pi/4$. With increasing the beam order, the magnitude of the longitudinal component of the angular momentum density increases. When the beam order is larger than 2, the increasing speed of the magnitude of the longitudinal component of the angular momentum density is dramatic. The profile of the longitudinal component of the angular momentum density is also slightly varied with changing the beam order. The influence of the Gaussian waist size on the distribution of the longitudinal component of the orbital angular momentum density is shown in Fig. 5 where $n = m = 3$ and $\alpha = \pi/4$. With increasing the Gaussian waist size, the magnitude and profile size of the longitudinal component of the orbital angular momentum density increase. However, the increasing speed of the magnitude of the longitudinal component of the orbital angular momentum density is slow with increasing the Gaussian waist size. In this case, therefore, the increase of the overall orbital angular momentum mainly stems from the expansion of profile size of the orbital angular momentum density. Finally, the effect of the linearly polarized angle on the distribution of the longitudinal component of the orbital angular momentum density is investigated, which is shown in Fig. 6. $w_0 = 5\lambda$ and $n = m = 3$ in Fig. 6. The linearly polarized angle only plays a role in the orientation of the longitudinal component of the orbital angular momentum density. With increasing the linearly polarized angle, the profile of

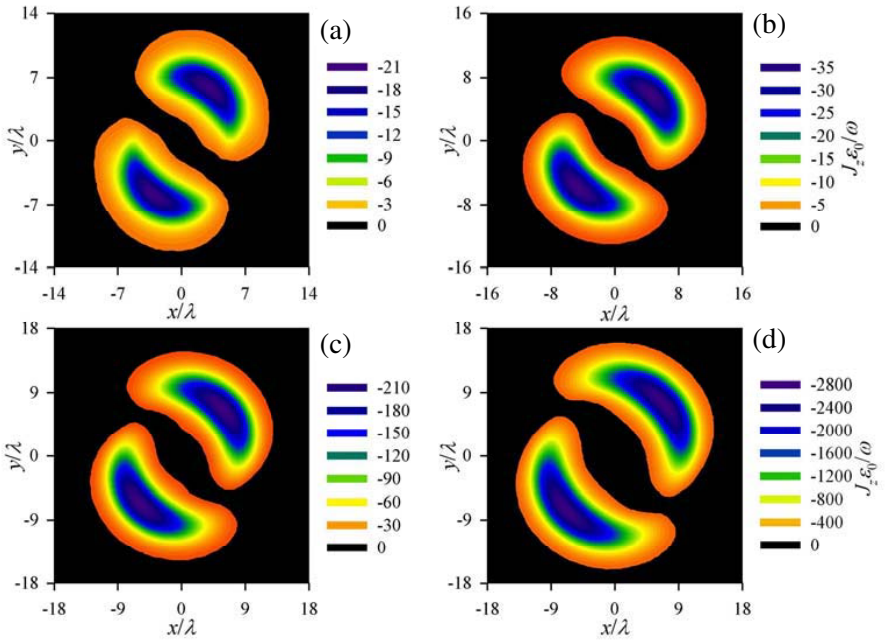

Figure 4. The longitudinal component of the orbital angular momentum density of a hollow vortex Gaussian beam in the reference plan $z = 25\lambda$. $w_0 = 5\lambda$, $m = 3$, and $\alpha = \pi/4$. (a) $n = 1$. (b) $n = 2$. (c) $n = 3$. (d) $n = 4$.

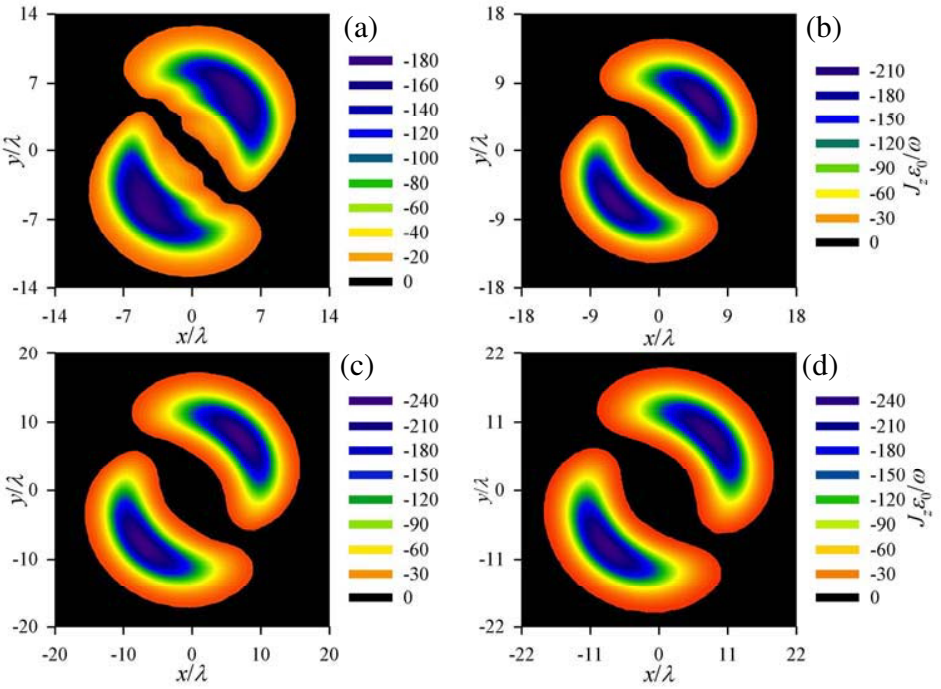

Figure 5. The longitudinal component of the orbital angular momentum density of a hollow vortex Gaussian beam in the reference plan $z = 25\lambda$. $n = m = 3$ and $\alpha = \pi/4$. (a) $w_0 = 4\lambda$. (b) $w_0 = 5\lambda$. (c) $w_0 = 6\lambda$. (d) $w_0 = 7\lambda$.

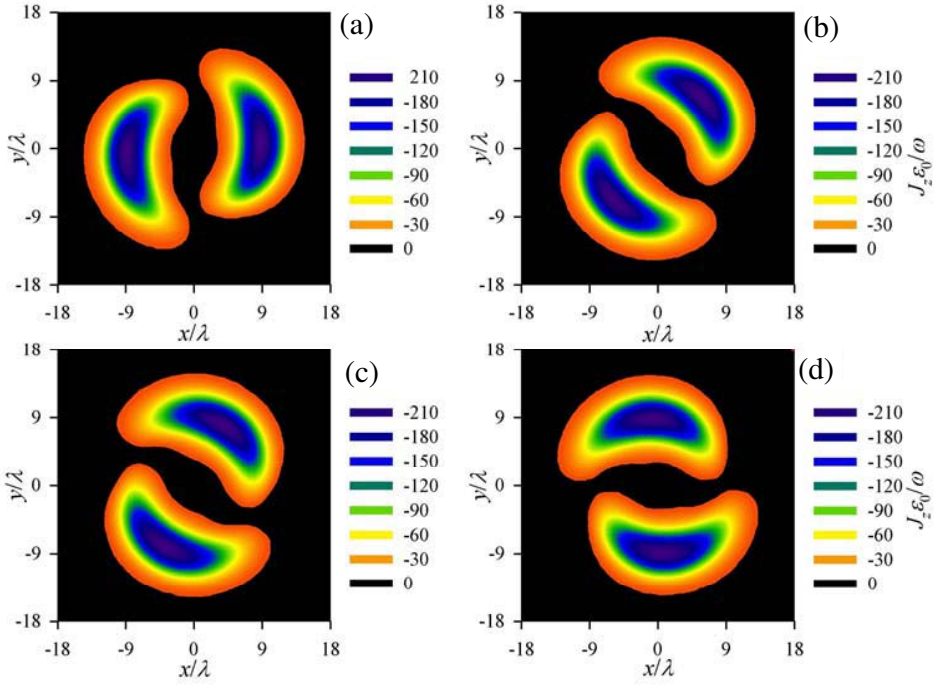

Figure 6. The longitudinal component of the orbital angular momentum density of a hollow vortex Gaussian beam in the reference plan $z = 25\lambda$. $w_0 = 5\lambda$ and $n = m = 3$. (a) $\alpha = 0$. (b) $\alpha = \pi/4$. (c) $\alpha = \pi/3$. (d) $\alpha = \pi/2$.

the longitudinal component of the orbital angular momentum density rotates a certain degrees counter clock wisely.

4. CONCLUSIONS

The starting point to describe the hollow vortex Gaussian beam is the Maxwell equations in free space. To obtain the exact solution of the Maxwell equations, the method of vectorial angular spectrum is employed. Based on the method of vectorial angular spectrum, analytical expressions of the electric and magnetic fields of a hollow vortex Gaussian beam propagating in free space are derived. By using the electromagnetic field of a hollow vortex Gaussian beam beyond the paraxial approximation, one can calculate and demonstrate the distribution of the orbital angular momentum density of a hollow vortex Gaussian beam in free space. As the overall transverse components of the orbital angular momentum are equal to zero, the effects of the topological charge, the beam order, the Gaussian waist size, and the linearly polarized angle on the distribution of longitudinal component of the orbital angular momentum density of a hollow vortex Gaussian beam are investigated. The linearly polarized angle only takes effect in the orientation of the longitudinal component of the orbital angular momentum density. Among the three parameters of the topological charge, beam order, and Gaussian waist size, longitudinal component of the orbital angular momentum density is most sensitive to the beam order and is least sensitive to the Gaussian waist size. With increasing the arbitrary one of the topological charge, beam order, and Gaussian waist size, the magnitude of the longitudinal component of the orbital angular momentum density increases. The above research is beneficial to the practical application of the hollow vortex Gaussian beam.

ACKNOWLEDGMENT

This research was supported by the National Natural Science Foundation of China under Grant Nos. 61178016 and 10974179.

REFERENCES

1. Yin, J., Y. Zhu, W. Jhe, and Y. Wang, "Atom guiding and cooling in a dark hollow laser beam," *Phys. Rev. A*, Vol. 58, 509–513, 1998.
2. Powell, P. N., "Blue-detuned dark-hollow laser guides atomic beam," *Laser Focus World*, Vol. 37, 58, 2001.
3. Wang, Z., Y. Dong, and Q. Lin, "Atomic trapping and guiding by quasi-dark hollow beams," *J. Opt. A: Pure Appl. Opt.*, Vol. 7, 147–153, 2005.
4. Yin, J., Y. Zhu, W. Wang, Y. Wang, and W. Jhe, "Optical potential for atom guidance in a dark hollow laser beam," *J. Opt. Soc. Am. B*, Vol. 15, 25–33, 1998.
5. Zhu, K., H. Tang, X. Sun, X. Wang, and T. Liu, "Flattened multi-Gaussian light beams with an axial shadow generated through superposing Gaussian beams," *Opt. Commun.*, Vol. 207, 29–34, 2002.
6. Cai, Y., X. Lu, and Q. Lin, "Hollow Gaussian beam and its propagation," *Opt. Lett.*, Vol. 28, 1084–1086, 2003.
7. Mei, Z. and D. Zhao, "Controllable dark-hollow beams and their propagation characteristics," *J. Opt. Soc. Am. A*, Vol. 22, 1898–1902, 2005.
8. Liu, Z., H. Zhao, J. Liu, J. Lin, M. A. Ahmad, and S. Liu, "Generation of hollow Gaussian beams by spatial filtering," *Opt. Lett.*, Vol. 32, 2076–2078, 2007.
9. Zheng, Y., X. Wang, F. Shen, and X. Li, "Generation of dark hollow beam via coherent combination based on adaptive optics," *Opt. Express*, Vol. 18, 26946–26958, 2010.
10. Schweiger, G., R. Nett, B. Özel, and T. Weigel, "Generation of hollow beams by spiral rays in multimode light guides," *Opt. Express*, Vol. 18, 4510–4517, 2010.

11. Ma, H., Z. Liu, F. Xi, and X. Xu, "Near-diffraction-limited dark hollow beam generated by using a hybrid control way," *Appl. Phys. B*, Vol. 105, 883–891, 2011.
12. Zhou, G., X. Chu, and J. Zheng, "Investigation in hollow Gaussian beam from vectorial structure," *Opt. Commun.*, Vol. 281, 5653–5658, 2008.
13. Chen, Y., Y. Cai, H. T. Eyyuboğlu, and Y. Baykal, "Scintillation properties of dark hollow beams in a weak turbulent atmosphere," *Appl. Phys. B*, Vol. 90, 87–92, 2008.
14. Deng, D. and Q. Guo, "Exact nonparaxial propagation of a hollow Gaussian beam," *J. Opt. Soc. Am. B*, Vol. 26, 2044–2049, 2009.
15. Gao, X., Q. Zhan, M. Yun, H. Guo, X. Dong, and S. Zhuang, "Focusing properties of spirally polarized hollow Gaussian beam," *Opt. Quant. Electron.*, Vol. 42, 827–840, 2011.
16. Sharma, A., M. S. Sodha, S. Misra, and S. K. Mishra, "Thermal defocusing of intense hollow Gaussian laser beams in atmosphere," *Laser and Particle Beams*, Vol. 31, 403–410, 2013.
17. MIshra, S. and S. K. Mishra, "Focusing of dark hollow Gaussian electromagnetic beams in a plasma with relativistic — Ponderomotive regime," *Progress In Electromagnetics Research B*, Vol. 16, 291–309, 2009.
18. Zhou, G., Y. Cai, and C. Dai, "Hollow vortex Gaussian beams," *Sci. China — Phys. Mech. Astron.*, Vol. 56, 896–903, 2013.
19. He, H., M. E. Friese, N. R. Heckenberg, and H. Rubinsztein-Dunlop, "Direct observation of transfer of angular momentum to absorptive particles from a laser beam with a phase singularity," *Phys. Rev. Lett.*, Vol. 75, 826–829, 1995.
20. Lee, W. M., X.-C. Yuan, and W. C. Cheong, "Optical vortex beam shaping by use of highly efficient irregular spiral phase plates for optical micromanipulation," *Opt. Lett.*, Vol. 29, 1796–1798, 2004.
21. Paterson, C., "Atmospheric turbulence and orbital angular momentum of single photons for optical communication," *Phys. Rev. Lett.*, Vol. 94, 153901, 2005.
22. Yao, A. M. and M. J. Padgett, "Orbital angular momentum: Origins behavior and applications," *Adv. Opt. Photon.*, Vol. 3, 161–204, 2011.
23. Cao, T. and M. J. Cryan, "Modeling of optical trapping using double negative index fishnet metamaterials," *Progress In Electromagnetics Research*, Vol. 129, 33–49, 2012.
24. Zhou, X., "On independence, completeness of Maxwell's equations and uniqueness theorems in electromagnetics," *Progress In Electromagnetics Research*, Vol. 64, 117–134, 2006.
25. Sha, W., X.-L. Wu, Z.-X. Huang, and M.-S. Chen, "Maxwell's equations, symplectic matrix, and grid," *Progress In Electromagnetics Research B*, Vol. 8, 115–127, 2008.
26. Gradshteyn, I. S. and I. M. Ryzhik, *Table of Integrals, Series, and Products*, Academic Press, New York, 1980.
27. Deng, D., S. Du, and Q. Guo, "Energy flow and angular momentum density of nonparaxial airy beams," *Opt Commun.*, Vol. 289, 6–9, 2013.
28. Zhou, G. and G. Ru, "Orbital angular momentum density of an elegant Laguerre-Gaussian beam," *Progress In Electromagnetics Research*, Vol. 141, 751–768, 2013.